Quantum Electronics **46** (3) 262–266 (2016)

FIBRE OPTICS

DOI: 10.1070/QEL15953

Influence of fibre structure and bends on optical cross-talk in multicore fibres

O.N. Egorova, M.S. Astapovich, L.A. Melnikov, M.Yu. Salganskii, V.P. Mishkin, K.N. Nishchev, S.L. Semjonov, E.M. Dianov

Abstract. **We have studied the influence of cross-sectional structure and bends on optical cross-talk in a multicore fibre. A reduced refractive index layer produced between the cores of such fibre with a small centre-to-centre spacing between neighbouring cores (27 μm) reduces optical cross-talk by 20 dB. The cross-talk level achieved, 30 dB per kilometre of the length of the multicore fibre, is acceptable for a number of applications where relatively small lengths of fibre are needed. Moreover, a significant decrease in optical cross-talk has been ensured by reducing the winding diameter of multicore fibres with identical cores.**

Keywords: *multicore fibres, optical cross-talk, bend sensitivity.*

1. Introduction

Even though multicore fibres were proposed as early as 1979 [1], potential applications for such fibres are only now beginning to emerge. The fibre transmission capacity of such fibres can be raised in proportion to the number of their cores, so they have attracted considerable interest due to their potential of increasing the transmission capacity of long-haul communication systems [2–4] and local access networks [5, 6]. The record high fibre transmission capacities achieved in recent years were ensured by 12-core (1 Pbit s^{-1} [7]) and 22-core (2.15 Pbit s^{-1} [8]) fibres. The use of multicore fibres instead of single-core fibres and ribbon cables will make it possible to simplify the design and maintenance of signal channels in data storage and processing centres and supercomputers [9, 10]. In a number of studies, multicore fibres were recently proposed for use in microwave photonics, namely, for producing multichannel delay lines [11] and multicavity optoelectronic oscillators [12]. In this case, the use of a multicore fibre instead of a set of individual single-core fibres makes it possible to reduce the influence of external factors [for example, that of the fibre geometry (macro- and microbends) and temperature difference] on parameters of devices, in particular on the group delay difference between channels. Multicore fibres are particularly attractive for applications where economy of space and the ability to reduce the number and weight of optical cables are critical. These are primarily on-board communication links and on-board equipment.

A key issue pertaining to the fabrication of multicore fibres is the ability to ensure both a large number of cores and low optical cross-talk. For a fibre to be mechanically strong and reliable, its diameter should not exceed 200–250 μm. Clearly, to increase the number of cores, the core spacing in the fibre cross section should be reduced, but this leads to an increase in optical cross-talk. To reduce cross-talk at a small core spacing, a layer with a reduced refractive index relative to the cladding is produced between the cores [13]. Located some distance from a core, such a layer reduces the electric field strength at the edge of the mode field distribution and the mode field overlap between neighbouring cores, leading to a reduction in cross-talk. At the same time, the reduced-index layer has no significant effect on the modal properties of individual cores.

In this report, we assess the effect of a reduced-index layer on optical cross-talk in multicore fibres. To this end, we have fabricated two multicore fibres having a small centre-to-centre spacing between the cores (27 μm), with and without a reduced-index layer. Our results demonstrate that, with this fibre design, the reduced-index layer decreases cross-talk by 20 dB per kilometre of the fibre length. The cross-talk level achieved is 30 dB km^{-1}. In addition, we show that reducing the fibre winding diameter reduces optical cross-talk in the fibre.

2. Influence of different factors on optical cross-talk

Light propagation through a multicore fibre is accompanied by interference of the mode fields of neighbouring cores, leading to transference of light from one core to another, i.e. to optical cross-talk [14]. The magnitude of this coupling is influenced by the structure of the fibre, its spatial position and longitudinal variations in its parameters.

Figure 1a shows a fibre cross section having seven guiding channels, which comprise cores (C1–C7), inner claddings (Cl1–Cl7) and a reduced-index layer (L). To assess the effect of the reduced-index layer, we calculated the mode field coupling coefficient and beat length (over which power is trans-

O.N. Egorova, M.S. Astapovich, S.L. Semjonov, E.M. Dianov Fiber Optics Research Center, Russian Academy of Sciences, ul. Vavilova 38, 119333 Moscow, Russia; e-mail: egorova@fo.gpi.ru;
L.A. Melnikov Yuri Gagarin State Technical University of Saratov, Politekhnicheskaya ul. 77, 410054 Saratov, Russia; V.A. Kotel'nikov Institute of Radio Engineering and Electronics (Saratov Branch), Russian Academy of Sciences, Zelenaya ul. 38, 410019 Saratov, Russia;
M.Yu. Salganskii G.G. Devyatykh Institute of Chemistry of High-Purity Substances, Russian Academy of Sciences, ul. Tropinina 49, 603950 Nizhnii Novgorod, Russia;
V.P. Mishkin, K.N. Nishchev N.P. Ogarev Mordovia State University, Bol'shevistskaya ul. 68, 430005 Saransk, Mordovian Republic, Russia

Received 22 October 2015; revision received 11 December 2015
Kvantovaya Elektronika **46** (3) 262–266 (2016)
Translated by O.M. Tsarev

ferred from one core to another and back again) in fibres with or without a reduced-index layer. The waveguiding system under consideration (Fig. 1b) comprises cores C1 and C2 (with a refractive index n_C), claddings Cl1 and Cl2 (with a refractive index n_{Cl}) and a reduced-index layer L (with a refractive index n_L). The refractive indices at a wavelength of 1550 nm are $n_C = 1.453$, $n_{Cl} = 1.444$ and $n_L = 1.435$.

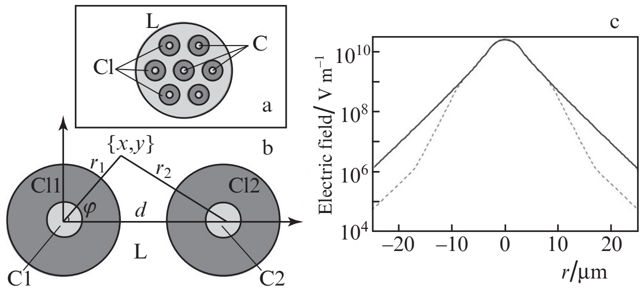

Figure 1. (a) Cross section of a multicore fibre, (b) waveguiding system under consideration and (c) mode field distributions across the fibres with (dashed line) and without (solid line) a reduced-index layer.

Power transfer between two cores can be evaluated using a coupled-mode equation [15, 16]:

$$\frac{\partial A_1}{\partial z} = -\,\mathrm{i}c_{21}\exp\left[-\mathrm{i}\int_0^z[\beta_2(z') - \beta_1(z')]\mathrm{d}z'\right]A_2,$$
$$\frac{\partial A_2}{\partial z} = -\,\mathrm{i}c_{12}\exp\left[-\mathrm{i}\int_0^z[\beta_1(z') - \beta_2(z')]\mathrm{d}z'\right]A_1. \qquad (1)$$

Here A_1 and A_2 are slowly varying mode field amplitudes of the C1 and C2 cores, respectively; c_{12} and c_{21} are the mode coupling coefficients for the C1 and C2 cores; z is a coordinate along the fibre axis; and $\beta_1(z')$ and $\beta_2(z')$ are the mode propagation constants of the respective cores at point z'.

Coupled equations for slowly varying amplitudes can also be obtained in the form [14, 17]

$$\frac{\partial A_1}{\partial z} - \mathrm{i}\frac{k^2 v_{12}}{2\beta_1 u_{11}}A_2 = 0,$$
$$\frac{\partial A_2}{\partial z} - \mathrm{i}\frac{k^2 v_{21}}{2\beta_2 u_{22}}A_1 = 0, \qquad (2)$$

where

$$u_{11} = \int_\infty \mathrm{d}S\,\Psi_1\Psi_1;$$

$$u_{22} = \int_\infty \mathrm{d}S\,\Psi_2\Psi_2;$$

$$v_{12} = (n_C^2 - n_L^2)\int_{C1}\mathrm{d}S\,\Psi_1\Psi_2 + (n_{Cl}^2 - n_L^2)\int_{C11}\mathrm{d}S\,\Psi_1\Psi_2;$$

$$v_{21} = (n_C^2 - n_L^2)\int_{C2}\mathrm{d}S\,\Psi_1\Psi_2 + (n_{Cl}^2 - n_L^2)\int_{Cl2}\mathrm{d}S\,\Psi_1\Psi_2;$$

Ψ_1 and Ψ_2 are the fields of partial modes of the C1 and C2 cores; and k is the wavenumber. It follows from these equations that the variation of the field amplitude in the cores has a period

$$L_p = \frac{4\pi\sqrt{\beta_1\beta_2 u_{11}u_{22}}}{k^2\sqrt{v_{12}v_{21}}}.$$

If the C1 and C2 cores are identical, we have $\beta_1 = \beta_2 = \beta$, $u_{11} = u_{22} = U$ and $v_{12} = v_{21} = v$. In addition, it follows from (1) and (2) that $c_{12} = c_{21} = c = k^2v/(2\beta U)$ and $L_p = 2\pi/c = 4\pi\beta U/(k^2v)$. The power variation period (beat length) is then $L_b = L_p/2 = \pi/c$. It is seen that the coupling coefficient is determined not only by the field overlap in the cores but also by the field overlap in the cladding region. The low-index region L reduces the field produced by the mode of the C2 core in the C1 core, i.e. reduces cross-talk between their modes [13].

Calculations were performed for cores with identical parameters. The following geometric parameters were used: core radii $R_{C1} = R_{C2} = R_C = 2.65$ μm, radii of the Cl1 and Cl2 inner claddings $R_{Cl} = 9.5$ μm and centre-to-centre spacing between the cores $d = 27$ μm. In integrating with respect to coordinates, R_{Cl} and d were normalised by R_C. The integration was performed numerically. To assess the effect of the reduced-index region, we considered two cases: $n_L = n_{Cl}$ and $n_L \neq n_{Cl}$.

At $n_L = n_{Cl}$, the characteristic frequency of an isolated waveguide is $V = 1.7346$ at a wavelength of 1550 nm. Solving the characteristic equation for a weakly guiding fibre [14, 17], we obtain $u = 1.4275$ and $w = 0.98532$ ($u^2 + w^2 = V^2$). The propagation constant is $\beta = \sqrt{k^2n_C^2 - u^2/R_C^2} = 5.8653$ μm^{-1}. We take the expression for $\Psi_{1,2}$ in a form typical of weakly guiding waveguides, which gives

$$U = 2\pi\int_0^1\left[\frac{J_0(ur)}{J_0(u)}\right]^2 r\mathrm{d}r + 2\pi\int_1^\infty\left[\frac{K_0(wr)}{K_0(w)}\right]^2 r\mathrm{d}r = 9.55614,$$

where J_0 and K_0 are the Bessel and Macdonald functions of zeroth order. To evaluate v, we use Eqn (37.81) from Ref. [17], which relates values of the Macdonald function in shifted coordinates (with respect to the centres of the cores; see Fig. 1b):

$$K_0(wr_2) = \sum_{p=-\infty}^{\infty}(-1)^p K_p(wd)I_p(wr_1)\cos(p\varphi), \qquad (3)$$

where I_p is a modified Bessel function and $r_2^2 = r_1^2 + d^2 - 2dr_1\cos\varphi$.

Since $n_{Cl} = n_L$, the expression for v includes only one integral over the Cl region. Integrating with respect to φ and substituting the expression for $K_0(wr_2)$ from (3), we obtain

$$v = 2\pi(n_C^2 - n_{Cl}^2)\int_0^1\frac{J_0(ur_1)}{J_0(u)}\frac{K_0(wd)I_0(wr)}{K_0(w)}r_1\mathrm{d}r_1 = 5.02624\times10^{-6}.$$

The coupling coefficient is then $c = k^2/(2\beta U) = 7.3678 \times 10^{-7}$ μm^{-1} and the beat length is $L_b = \pi/c \approx 4.3$ m.

At $n_L \neq n_{Cl}$, to evaluate the beat length and coupling coefficient we should find the fundamental mode field in a weakly guiding bilayer waveguide. To this end, we represent the fields in the core, cladding and the medium between the claddings in the form [18]

$$E_x(x,y) = \begin{cases} AJ_0(ur), & r \leqslant 1, \\ BK_0(wr) + CI_0(wr), & 1 < r \leqslant R_{Cl}, \\ DK_0(qr), & r > R_{Cl}, \end{cases}$$

and make up connection conditions for the field and its derivatives:

$$
\begin{aligned}
&AJ_0(u) = BK_0(w) + CI_0(w),\\
&BK_0(wR_{\rm Cl}) + CI_0(wR_{\rm Cl}) = DK_0(qr),\\
&-UAJ_1(u) = -wBK_1(w) + wCI_1(w),\\
&-wBK_1(wR_{\rm Cl}) + wCI_1(wR_{\rm Cl}) = -qDK_1(qR_{\rm Cl}),
\end{aligned} \tag{4}
$$

where $u^2 = R_{\rm C}^2(k^2n_{\rm C}^2 - \beta^2)$; $-w^2 = R_{\rm C}^2(k^2n_{\rm Cl}^2 - \beta^2)$; $-q^2 = R_{\rm C}^2(k^2n_{\rm L}^2 - \beta^2)$; $-q^2 + w^2 = V_0^2$.

A nontrivial solution exists if the determinant of system (4) is zero. This equation, in combination with the coupling equations for u, w and q, offers the possibility of determining these parameters and the propagation constant. We obtain $u = 1.42861$, $w = 0.983761$, $q = 1.99411$ and $\beta = 5.86526$ μm^{-1}. It is seen that the propagation constant β remained essentially unchanged, along with the parameters u and w. At the same time, the field falls off more rapidly in the reduced-index layer than in the cladding ($q \approx 2 > w$). The coefficients A, B, C and D can be determined from system (4). Using their values $A = 1$, $B = 1.282494$, $C = -0.001108$ and $D = 44.226722$, we can find the field distribution. Integrating, we obtain $c = 2.132 \times 10^{-8}$ μm^{-1} and $L_{\rm b} \approx 150$ m. Thus, c decreased by more than one order of magnitude relative to that in the absence of a reduced-index layer.

The above calculations were verified numerically by the finite element method using COMSOL Multiphysics software. The calculation results obtained by the two methods coincide. Figure 1c shows the mode field distribution plotted on a logarithmic scale for a core with and without a reduced-index region. It is seen that, at $n_{\rm L} < n_{\rm Cl}$, the field strength at the edges of the mode field distribution is considerably lower than that in the case where there is no reduced-index layer. The decrease in field strength at the edges of the mode field distribution makes it possible to reduce the coupling coefficient c and beat length $L_{\rm b}$.

It is worth noting, however, that the above calculation takes into account neither random fluctuations in parameters of the fibre along its length nor the effect of fibre position on cross-talk, so it provides only a qualitative picture of how the reduced-index layer influences the cross-talk level.

Cross-talk is significantly influenced not only by the cross-sectional fibre structure but also by the spatial position of the fibre, i.e. by bends and rotations of the fibre about its axis. Figure 2a shows a multicore fibre bent about the z axis, and Fig. 2b presents the refractive index profile of a straight fibre along the x axis. Since all the cores of the fibre are identical, they have identical propagation constants (β) and identical effective mode indices ($n_{\rm eff} = \beta/k$). In the refractive index profile, $n_{\rm eff}$ is indicated by a dashed line. A bent fibre is known to be equivalent to a straight fibre with an effective index profile [19]

$$
n_{\rm eff}^2 = n^2\Big(1 + 2\frac{r}{R}\cos\theta\Big), \tag{5}
$$

where r and θ are the coordinates of the point at which we determine the refractive index (in a local cylindrical coordinate system); n is the refractive index of a straight fibre at point (r, θ); and R is the bend radius. Figure 2c shows the equivalent refractive index profile of the bent fibre along the x axis ($\theta = 0$). The bent fibre has a tilted refractive index profile [according to (5), the slope increases with decreasing bend radius]. Bending the multicore fibre with identical cores is seen to cause a difference in $n_{\rm eff}$ between neighbouring modes. According to (1), increasing the difference reduces cross-talk. Thus, whereas a straight multicore fibre has identical mode $n_{\rm eff}$'s, the modes of individual cores in a bent fibre are phase-mismatched, leading to a reduction in optical cross-talk. In a fibre with different core parameters, the opposite situation may occur: if neighbouring cores differ in mode $n_{\rm eff}$ in a straight fibre, at a certain bend direction the effective mode index difference may decrease to the extent that the phase matching condition will be met and optical cross-talk will rise sharply.

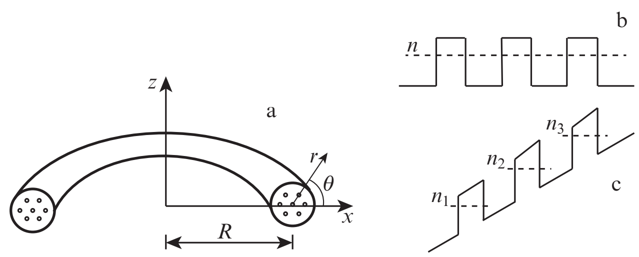

Figure 2. (a) Multicore fibre bent to a radius R and refractive index profiles of (b) a straight and (c) a bent fibre.

The slope of the refractive index profile and, hence, the mode $n_{\rm eff}$ difference are determined not only by the fibre bend radius R but also by the angle θ [Fig. 2a, Eqn (5)]. Clearly, the bend-induced change in the cross-talk between the central core and the cores whose centres lie on the x axis will be greater than that in the cross-talk between the central core and the other four cores.

Fibre bends may lead not only to controlled changes in cross-talk, e.g. when fibre is wound at a constant diameter or when the orientation of the fibre cross section relative to the bend direction is retained throughout the length of the fibre, but also to a random scatter in optical cross-talk because, under real service conditions, variations in R and θ along the fibre length are uncontrolled [20].

There are also other factors responsible for uncontrolled changes in optical cross-talk. In particular, in the fibre fabrication process there are always small variations in the diameter and refractive index of the cores along the length of the fibre [21]. As a result, in a fibre with identical cores phase mismatch between modes of neighbouring cores and, as a consequence, random variations in cross-talk are possible. Moreover, fibre microbends may lead to transference of light through cladding modes of neighbouring cores, that is, light will first leak out of a mode of one core to cladding modes, which will then interact with modes of other cores [22].

3. Fabrication and characterisation of fibres

Multicore fibre preforms were assembled using pure silica rods and rods produced from single-core preforms. To produce a fibre with a reduced-index layer, preforms with a germania-doped core were jacketed in a fluorinated silica tube with a refractive index lower than that of undoped SiO_2. A fluorinated silica layer was produced by MCVD. Rods obtained by drawing a preform with a GeO_2-doped core and pure silica rods were stacked and placed in a silica tube. Next, the preform stack was consolidated into a solid preform rod by heating in a furnace at 2000°C at a reduced pressure in the tube. The preforms were drawn into fibres.

Figure 3 shows atomic force microscopy images of the central part of the fibre end faces. The fibre end faces were first etched with hydrofluoric acid. Since the etch rate of silica glass depends on its composition (dopant concentration), the surface topography of the fibre end face reflects the glass composition, which allowed us to gain information about the fibre cross section geometry.

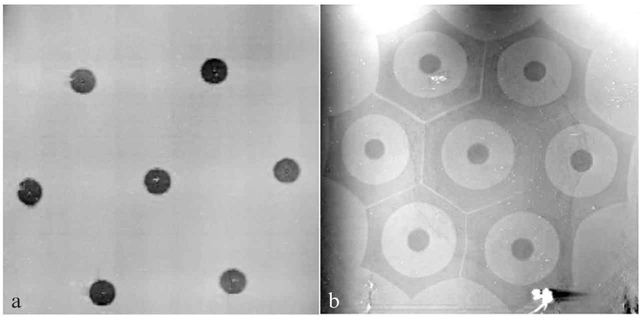

Figure 3. Atomic force microscopy images of the end faces of the fibres (a) without and (b) with a reduced-index layer.

Both fibres had seven cores, which were produced from the same preform and had identical parameters. The centre-to-centre spacing between neighbouring cores was 27 μm, the core diameter was 5.3 μm, and the core–cladding refractive index difference was 0.009. One of the fibres contained a reduced-index fluorinated silica layer 8–9 μm in thickness (along the line connecting the centres of neighbouring cores). Its refractive index was lower than that of the cladding by 0.009. The cladding diameter within the fluorinated layer was 19 μm.

The cutoff wavelength was determined by comparing the power transmitted through a straight segment of the fibre under investigation and the power transmitted through a multicore fibre segment. To measure the first higher order mode cutoff wavelength and mode field diameter, light was coupled into each of the cores under investigation using a butt-joined single-core fibre. The cutoff wavelengths thus found ranged from 1200 to 1210 nm in the fibre with no reduced-index layer and from 1300 to 1400 nm in the fibre with such a layer. The shift of the cutoff wavelength is obviously due to additional first higher order mode field localisation by the reduced-index layer. At a wavelength of 1.3 μm, the mode field diameter in the different cores was about 6 μm.

To measure cross-talk, a signal at a wavelength of 1.55 μm was launched into the central core by butting it against a lead-in single-mode, single-core fibre. The power at the output of the cores of the multicore fibre was measured by scanning the fibre end face with a single-mode fibre connected to a photodetector. The length of the fibre with a reduced-index layer was 1.1 km, and that of the fibre with no such layer was 1.0 km. The measurements were made at fibre winding diameters of 32, 16 and 5 cm. The cross-talk level was evaluated as the ratio of the output powers of the peripheral and central cores.

Figure 4 illustrates the effect of fibre winding diameter on the cross-talk in the fibres. It is seen that, at a given fibre bend diameter, the scatter in optical cross-talk is 10–15 dB. The scatter may originate from the effect of fibre winding conditions: changes in the orientation of the fibre cross section relative to the bend direction, microbends and random variations in parameters of the fibre along its length.

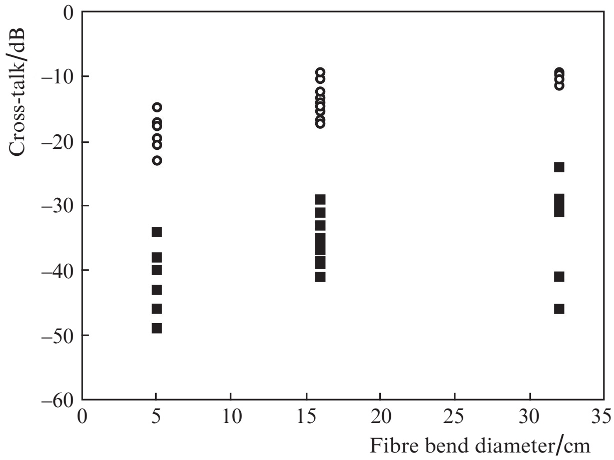

Figure 4. Cross-talk between the central and peripheral cores as a function of fibre bend diameter for the fibres with (■) and without (○) a reduced-index layer.

The optical cross-talk level in the fibre with a reduced-index layer was on average 20 dB lower than that in the fibre with no such layer. At a fibre winding diameter of 16 cm, the average cross-talk levels in the fibres with and without a reduced-index layer were –35 and –15 dB, respectively.

The optical cross-talk level in both fibres decreases with decreasing bend diameter (Fig. 4) because, as follows from (5), this is accompanied by an increase in the slope of the equivalent refractive index profile, leading to an increase in the mode n_{eff} difference between neighbouring cores. As the fibre bend diameter decreases from 16 to 5 cm, the cross-talk level drops, on average, by 5 dB.

4. Conclusions

Multicore fibres having a centre-to-centre spacing between neighbouring cores of 27 μm and a reduced-index layer have been fabricated and investigated. Comparison of the properties of the fibres demonstrates that such a layer allows optical cross-talk to be reduced but causes no significant changes in cutoff wavelength or mode field diameter. The cross-talk between the cores in the fibre having the reduced-index layer is 30 dB km^{-1}, which is acceptable for a number of applications where the fibre length does not exceed one or a few kilometres (for example, in on-board equipment). We have studied the effect of fibre bend diameter on the cross-talk level. With decreasing fibre bend diameter, the optical cross-talk level decreases because of the associated increase in the difference between the mode propagation constants of neighbouring cores.

Acknowledgements. This work was supported in part by the Russian Foundation for Basic Research (Grant No. 14-29-08183).

References

1. Inao S., Sato T., Sentsui S., Kuroha T., Nishimura Y. *OFC 1979 Conf. Papers* (Washington, 1979) WB1.
2. Sakaguchi J., Awaji Y., Wada N., Hayashi T., Nagashima T., Kobayashi T., Watanabe M. *OFC 2011 Conf. Papers* (Los Angeles, 2011) OWJ2.
3. Sakaguchi J., Puttnam B.J., Klaus W., Awaji Y., Wada N., Kanno A., Kawanishi T., Imamura K., Inaba H., Mukasa K., Sugizaki R., Kobayashi T., Watanabe M. *OFC 2012 Conf. Papers* (Los Angeles, 2012) PDP5C.1.
4. Zhu B., Taunay T.F., Fishteyn M., Liu X., Chandrasekhar S., Yan M.F., Fini J.M., Monberg E.M., Dimarcello F.V. *Opt. Express*, **19**, 16665 (2011).
5. Rosinski B., Chi J.D., Grosso P., Bihan J.L. *J. Lightwave Technol.*, **17**, 807 (1999).
6. Zhu B., Taunay T.F., Yan M.F., Fishteyn M., Oulundsen G., Vaidya D. *IEEE Photonics Technol. Lett.*, **22**, 1647 (2010).
7. Takara H., Sano A., Kobayashi T., Kubota H., Kawakami H., Matsuura A., Miyamoto Y., Abe Y., Ono H., Shikama K., Goto Y., Tsujikawa K., Sasaki Y., Ishida I., Takenaga K., Matsuo S., Saitoh K., Koshiba M., Morioka T. *Proc. ECOC 2012* (Amsterdam, 2012) Th.3.C.1.
8. Puttnam B.J., Luis R.S., Klaus W., Sakaguchi J., Mendinueta J.-M.D., Awaji Y., Wada N., Tamura Y., Hayashi T., Hirano M., Marciante J. *ECOC 2015* (Valencia, 2015) PDP 3.1.
9. Berthold J. *OFC 2012 Conf. Papers* (Los Angeles, 2012) OW1J.1.
10. Taubenblatt M. *OFC 2011 Conf. Papers* (Los Angeles, 2011) OThH3.
11. Gasulla I., Capmany J. *IEEE Photonics J.*, **4**, 877 (2012).
12. Garcia S., Gasulla I. *Opt. Express*, **23**, 2403 (2015).
13. Dianov E.M., Egorova O.N., Semjonov S.L. WO 2012/099498 A2.
14. Snyder A.W., Love J.D. *Optical Waveguide Theory* (London: Chapman and Hall, 1983; Moscow: Radio i Svyaz', 1987).
15. Snyder A.W. *J. Opt. Soc. Am.*, **62**, 1267 (1972).
16. Hayashi T., Taru T., Shimakawa O., Sasaki T., Sasaoka E. *Opt. Express*, **19**, 16576 (2011).
17. Marcuse D. *Integrated Optics* (New York: IEEE, 1973; Moscow: Mir, 1974).
18. Adams M. *An Introduction to Optical Waveguides* (New York: Wiley, 1981; Moscow: Mir, 1984).
19. Marcuse D. *Appl. Opt.*, **21**, 4208 (1982).
20. Fini J.M., Zhu B., Taunay T.F., Yan M.F. *Opt. Express*, **18**, 15122 (2010).
21. Takenaga K., Tanigawa S., Guan N., Matsuo S., Saitoh K., Koshiba M. *OFC 2010 Conf. Papers* (San Diego, Cal., 2010) OWK7.
22. Li S., Butler D.L., Li M.-J., Koklyushkin A., Nazarov V., Khrapko R., Geng Y., McCollum R.L. *IPC 2013* (Bellevue, WA, 2013) TuF3.2.